

## NOTE

# Surfactant-Assisted Synthesis of Mesoporous Zirconia Powders with High Surface Areas

Since the advent of mesoporous aluminosilicates (1), the possibility of producing similar structures with other metal oxides has attracted considerable attention. Stucky and co-workers (2) reported on the synthesis of tungsten, iron, and tin mesostructures, but attempts to remove the surfactant caused the pore structure to collapse. Antonelli and Ying (3) produced the first non-aluminosilicate-based mesoporous material that remained stable upon removal of the organic surfactant. They used tetradecylphosphate as the organic template and titanium isopropoxide partially substituted with acetylacetone as the metal source. Knowles and Hudson (4) recently showed that alkylammonium salts can be used to prepare zirconia in the mesoporous range, and they pointed out that the conventional mechanism of mesopore formation does not take place in this cationic surfactant–metal cation pair.

Zirconia is an excellent catalyst support (5–8). There is also abundant catalysis literature in the area of strong, zirconia-based solid acids (9–14). The surface areas obtained by conventional precipitation of zirconyl salts with ammonia are typically in the 80–140 m<sup>2</sup>/g range after activation under flowing air at 823–923 K. Aerogels with high surface areas can be prepared (15, 16), but they are synthesized from moisture sensitive precursors, and low-pressure separations of organic solvents from the precipitation media are also necessary. Our working hypothesis was that if a classical anionic surfactant/cationic precursor route were to be implemented to synthesize mesoporous zirconia, the preparation scheme should then be geared toward the synthesis of active catalysts, i.e., by using the adequate surfactant and/or surfactant removal steps. By the time we submitted this contribution, Schüth *et al.* (17) had reported on the synthesis of mesoporous zirconia systems using a synthetic scheme similar to that proposed by Antonelli and Ying (3). Their mesostructures showed to collapse at temperatures above 500°C.

One synthesis route that produced catalysts with very good isomerization activity consisted of mixing a solution of 3 g of lauryl sulfate (sodium form) in 10 ml conc. NH<sub>3</sub>, 1 ml acetylacetone (acac), and 5 ml ethanol, with a saturated solution of ZrOCl<sub>2</sub> · 8H<sub>2</sub>O (2.20 g salt). The mixture was stirred vigorously for 5 min, then transferred to a pressure

tube and placed in an oven at 383 K for 6 h. The precipitate was then washed thoroughly with water and ethanol. In order to completely remove the surfactant and to load this catalyst precursor with sulfate ions, we proceeded to suspend 200 mg of the dried powders in a solution of 200 mg of (NH<sub>4</sub>)<sub>2</sub>SO<sub>4</sub> dissolved in 3.6 ml ethanol and 3 ml water. This suspension was placed in a sealed vial and kept in an oven at 383 K for another 6 h. Once filtered, washed again with ethanol, and dried at 110°C, the sample was redried *in vacuo* at 403 K for 30 min to perform BET surface area measurements. The adsorption apparatus has been described earlier (18). This sample, labeled as SZ-403, had a BET surface area of 425 m<sup>2</sup>/g (a second batch gave a surface area of 397 m<sup>2</sup>/g). In the absence of surfactant, we obtained a sample with a BET surface area of 345 m<sup>2</sup>/g after oven drying. The Dollimore method (19) for pore size analysis was applied to the desorption curves of both blank and catalyst samples (Fig. 1). This pore size distribution method is known to perform well for pore sizes larger than 20 Å. The blank samples were made by excluding the surfactant from the precipitation media. Our four samples were labeled SZ-403, SZ-848, bSZ-403, and bSZ-848, with the suffix corresponding to the calcination temperature (K) and the “bl” prefix to “blank.”

Zirconia is microporous upon precipitation in the absence of surfactants (pores <20 Å), but calcination results in broad pore distributions (20). Figure 1 shows that upon calcination, the blank sample produces pores above 20 Å, but it is the presence of surfactant during the precipitation step that results in much sharper mesoporosity features. The pore sizes are in the 24–26 Å range for SZ-403, but they decrease in magnitude and shift toward slightly larger values upon calcination (SZ-848 sample).

Our choice of surfactant and surfactant concentration was not in any way arbitrary. We chose lauryl sulfate because its polar head group could have resulted in the one-step synthesis of mesoporous sulfated zirconia catalyst without further synthetic (wet) steps. We later found that such catalyst showed low activity for *n*-butane isomerization, presumably due to the presence of residual sodium ions (from the surfactant) on the catalyst surface. This led us to implement the surfactant washing/sulfate loading step

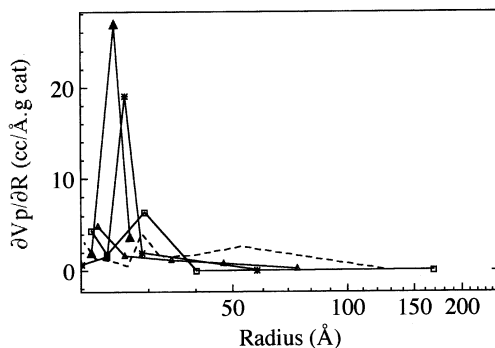


FIG. 1.  $\partial V_p/\partial R$  vs  $R$  curves for (\*) SZ-403, (▲) SZ-403 again around the 20–30 Å range, (- - -) b1SZ-848, (△) b1SZ-403, and (□) SZ-848.

discussed above. We also used high surfactant concentrations because a spherical-to-rod transition in the lauryl sulfate micelle shape is expected above 20 wt% (21), but we have not systematically studied the effect of micelle concentration and pH to test this hypothesis.

The X-ray diffraction measurements were performed as described previously (22). Between  $2\theta = 1^\circ$  and  $10^\circ$ , a broad shoulder was found around  $2-3^\circ$ , but this feature disappeared after washing and calcination (Fig. 2). We reproduced the XRD and desorption features several times to rule out the occurrence of artifacts. Using aging times up to 90 h did not lead to improvement of this broad shoulder in low-angle XRD pattern. Upon calcination at 848 K, this feature disappears, giving rise to broad tetragonal zirconia XRD signals, but the pore size distribution analysis still indicates that mesoporosity was not lost (S.A. of the SZ-848 catalyst:  $215 \text{ m}^2/\text{g}$ ). It is apparent that a pore formation mechanism that differs from that of MCM materials may be in effect, in which pore size uniformity does not necessarily imply bi- or three-dimensional X-ray detectable ordering.

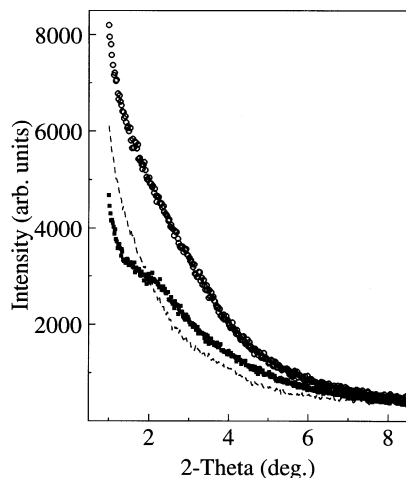


FIG. 2. Low-angle XRD patterns of SZ-403 (■) prior to washing, (○) after  $\text{SO}_4=$  loading/washing and (- - -) after calcination.

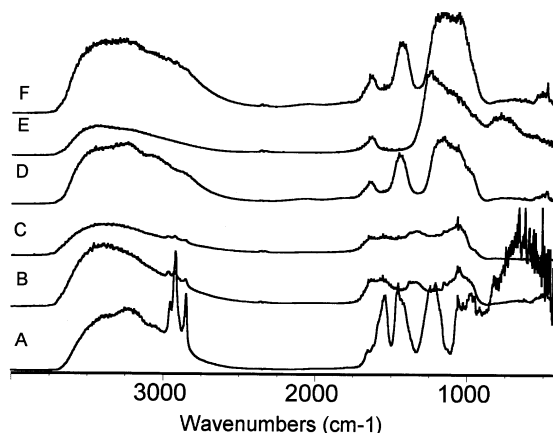


FIG. 3. DRIFTS spectra of SZ-403 (A) prior to washing, (B) washed with  $\text{H}_2\text{O}$ , (C) washed with EtOH, (D) after  $\text{SO}_4=$  loading, SZ-848 (E) after reaction, and (F)  $\text{SO}_4=$  loaded blank.

Figure 3 shows the background-subtracted DRIFTS spectra of the samples at different preparation stages. Our DRIFTS apparatus has been described previously (18). Note that the C–H stretching region is completely washed out after the second step (sulfate-loading, D spectrum). Multiplicity in the hydroxyl region is expected to be the result of both water and ethanol being present upon drying of the sample at low temperatures. We have previously discussed the  $1500$  and  $1400 \text{ cm}^{-1}$  bands in terms of hydration of sulfate groups and S=O moieties (22). Note that only the  $1400 \text{ cm}^{-1}$  band disappears after calcination, leaving the well-known IR features observed in sulfated zirconia catalysts (spectrum E). The lauryl-free, blank sample (once loaded with sulfate, and prior to calcination) showed a DRIFTS spectrum comparable to that of the washed mesoporous sample (spectra F and D).

As shown in Fig. 4, SZ-848 showed good activity for *n*-butane isomerization and disproportionation at 483 K. The rate ( $\text{g } n\text{-C}_4 \text{ converted}/\text{g catalyst}\cdot\text{h}$ ) is reported as a

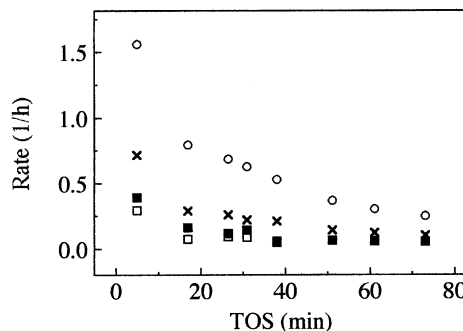


FIG. 4. Rate vs time on stream curves for the *n*-butane isomerization reaction over SZ-848 at 483 K. Packed-bed, atmospheric reactor.  $\text{Pn-C}_4 = 101.3 \text{ kPa}$ . Total conversion:  $<3.5\%$ . (○) isobutane, (×) isopentane  $\times 10$ , (■) propane  $\times 10$ , and (□) *n*-pentane  $\times 10$ .

function of time on stream to provide the reader with a reference point for comparison with the abundant literature on *n*-butane isomerization over sulfated zirconia catalysts. Under differential reactor operation (total % Conv <3.5), the bLSZ-848 catalyst had a lower initial activity than that of SZ-848, but this may be due to its lower starting surface area. For example, the relative activities ( $A_{\text{SZ-848}}/A_{\text{bLSZ-848}}$ ) under the same T, P, and WHSV, after 5 and 70 min on stream were 4.3 and 0.69, respectively. The SZ-848 sample also maintains, or slightly increases, its isopentane-to-isobutane ratio throughout the kinetic run (from 0.048 to 0.059 at 5 and 70 min TOS respectively), but the blank, bLSZ-848 catalyst, followed an opposite trend (0.071 to 0.049 at 5 and 70 min TOS respectively). It is conceivable that the larger population of mesopores in SZ-848 causes the disproportionation pathway (which is bimolecular in nature) to remain important at longer times on stream. On the other hand, the isomerization route has been suggested to be strictly bimolecular (23), but also to be a convolution of intra- and intermolecular processes (24). The effect of pore structure on the selectivity and deactivation of sulfated zirconia has not, to the best of our knowledge, been addressed. *A priori*, we expect the bimolecular mechanisms that lead to both disproportionation of *n*-butane and deactivation to be favored by larger pores. In a future contribution, we will investigate the effect of surfactant chain length on these parameters.

In summary, our results suggest that the porosity of sulfated zirconia can also be tailored by means of relatively simple synthetic routes, a fact that may well lead to changes in product selectivity and deactivation profiles. The micelle structure (cylinder vs sphere) and its role in catalyst pore structure still needs to be addressed, and we are planning to obtain TEM images of our samples in the near future.

#### ACKNOWLEDGMENT

We gratefully acknowledge support from the NSF (CTS-940618).

#### REFERENCES

1. Kresge, C. T., Leonowicz, M. E., Roth, W. J., Vartulli, J. C., and Beck, J. S., *Nature* **359**, 710 (1992).

2. Ciesla, U., Demuth, D., Leon, R., Petroff, P., Stucky, G., Unger, K., and Schüth, F., *J. Chem. Soc. Chem. Commun.*, 1387 (1994).
3. Antonelli, D. M., and Ying, J. Y., *Angew. Chem. Int. Ed. Engl.* **34**, 2014 (1995).
4. Knowles, J. A., and Hudson, M. J., *J. Chem. Soc. Chem. Commun.*, 2083 (1995).
5. Marti, P. E., Maciejewski, M., and Baiker, A., *J. Catal.* **139**, 494 (1993).
6. Amenomiya, Y., *Appl. Catal.* **30**, 347 (1987).
7. Dalla Betta, R. A., Piken, A. G., and Shelef, M., *J. Catal.* **40**, 173 (1975).
8. Bruce, L. A., and Mathews, J. F., *Appl. Catal.* **4**, 353 (1982).
9. Adeeva, V., de Haan, J. W., Jänchen, J., Lei, G. D., Schünemann, V., van de Ven, L. J. M., Sachtler, W. M. H., and van Santen, R. A., *J. Catal.* **151**, 364 (1995).
10. Cheung, T.-K., d'Itri, J. L., and Gates, B. C., *J. Catal.* **151**, 464 (1995).
11. Ebitani, K., Konno, H., Tanaka, T., and Hattori, H., *J. Catal.* **135**, 60 (1992).
12. Iglesia, E., Soled, S. L., and Kramer, G. M., *J. Catal.* **144**, 238 (1993).
13. Hino, H., *Chem. Lett.*, 971 (1989).
14. Hino, M., and Arata, K., *Catal. Lett.* **30**, 25 (1995).
15. Ward, D. M., and Ko, E. I., *J. Catal.* **150**, 18 (1994).
16. Teichner, S. J., Nicolaon, G. A., Vicarini, M. A., and Gardes, G. E. E., *Adv. Colloid Interf. Sci.* **5**, 245 (1976).
17. Schüth, F., Ciesla, U., and Schacht, S., *Angew. Chem.* **35**, 541 (1996).
18. Larsen, G., Lotero, E., Márquez, M., and Silva, H. S., *J. Catal.* **157**, 645 (1995).
19. Dollimore, D., and Heal, G. R., *J. Colloid Interf. Sci.* **33**, 508 (1970).
20. Mercera, P. D. L., van Ommen, J. G., Doesburg, E. B. M., Burggraaf, A. J., and Ross, J. R. H., *Appl. Catal.* **57**, 127 (1990).
21. Husson, R., and Luzzatti, L., *J. Phys. Chem.* **68**, 3504 (1964).
22. Larsen, G., Lotero, E., Raghavan, S., Parra, R. D., and Querini, C. A., *Appl. Catal. A: Gral.*, in press.
23. Adeeva, V., Lei, G. D., and Sachtler, W. M. H., *Appl. Catal. A: Gral.* **118**, L11 (1994).
24. Garin, F., Seyfried, L., Girard, P., Maire, G., Abdulsamad, A., and Sommer, J., *J. Catal.* **151**, 26 (1995).

Gustavo Larsen  
Edgar Lotero  
Mark Nabity  
Lucia M. Petkovic  
David S. Shobe

Department of Chemical Engineering  
University of Nebraska  
Lincoln, Nebraska 68588-0126

Received May 9, 1996; revised July 25, 1996; accepted July 26, 1996